

Frequency-Mismatch-Tolerant Silicon Vibratory Gyroscope without Vacuum Package for Automotive Applications

¹Huisui Zhang, ¹Qiang Zou, ¹Eun Sok Kim, ²Asad M. Madni, ²Lynn E. Costlow
and ²Roger F. Wells

¹*Department of Electrical Engineering-Electrophysics
University of Southern California
Los Angeles, CA 90089-0271 U.S.A.*

Tel: (213) 740-4697 Fax: (213) 740-8677 Email: eskim@mizar.usc.edu

²*BEI Technologies, Inc.*

13100 Telfair Avenue, Sylmar, California 91342 U. S. A.

Tel: (818) 364-7215 Fax: (818) 362-1836

E-Mail: beimadni@aol.com lcostlow@systron.com r wells@bei-tech.com

ABSTRACT

This paper describes a low-cost silicon vibratory gyroscope that tolerates a relatively large mismatch between the driving-mode and sensing-mode frequencies. The gyroscope is based on beam-mass structure and realized by one silicon proof mass and two beams for the driving and sensing mode. Piezoelectric actuation is used to produce a large driving mode vibration displacement (about 100 μm) with about 32 $V_{\text{peak-to-peak}}$. Two tiny sensing beams are separated from the vertical silicon beam to increase the sensitivity while keeping the sensing-mode resonant frequency high. Piezoresistive and piezoelectrical sensing mechanisms are applied to two different gyroscopes. The gyroscope operating at 1-4 kHz is capable of sub-degree-per-second angular rate sensitivity without any vacuum package.

KEYWORDS: Gyroscope, Piezoelectric Actuation, Frequency Match, Frequency Tolerance

1. INTRODUCTION

Inertial sensors including accelerometer and gyroscope are used in safety-critical applications in automobiles [1]. Because of the compact size and low cost, MEMS silicon inertial sensors have already been widely used in the automotive control electronics, such as air-bag deployment sensing system, vibration compensation, roll-over and stability control system [2-3]. To increase the sensitivity, the vibratory gyroscope, which is usually based on the Coriolis effect, requires high quality factor (Q) for the sensing mode vibration, which is usually achieved by vacuum package [4-5]. However, extremely high Q causes the vibration amplitude to degenerate greatly even at very nearby frequencies. Thus, accurate match between the driving-mode and sensing-mode resonant frequencies is required, and is a challenge for the current gyroscope design and fabrication [6-7].

In the current automotive application, the driving voltage available is usually as low as several volts. It is difficult to obtain large driving vibration amplitude from such a low voltage by electrostatic actuation. Piezoelectric actuation, however, has the potential to provide powerful driving ability at a low drive voltage.

In this paper, a piezoelectric driving gyroscope, with a novel sensing beam topology, is reported. It can provide sub-degree-per-second sensitivity in ambient pressure, and requires no vacuum package. The gyroscope is based on relatively low quality factor in air, and is tolerant to frequency mismatch between the driving and sensing vibration frequencies.

2. GYROSCOPE DESIGN

The gyroscope is based on a beam-mass structure. As illustrated in Figure 1, the gyroscope is driven to vibrate in the Z-axis direction by the piezoelectric unimorph. An angular rate (Ω) in the X-axis produces Coriolis force along the Y-axis, which results in the sensing-mode acceleration. A vertical silicon beam is designed to match the sensing-mode frequency to the driving-mode frequency. Two tiny sensing beams are placed symmetrically next to the vertical beam to pick up the sensing-mode vibration. The tiny sensing beams are either ion-implanted silicon beams (for piezoresistive sensing) or ZnO-deposited parylene beams (for piezoelectric sensing).

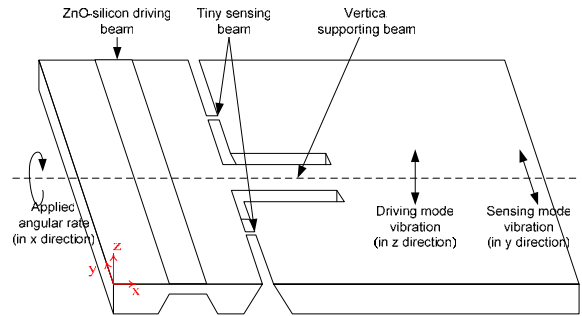


Figure 1. Schematic illustration of the working principle of the gyroscope

The driving mode vibration, sensing mode vibration and stress distribution are simulated with Finite Element Analysis (ALGOR), and are shown in Figure 2. The tiny sensing beams ($20 \times 2 \times 3 \mu\text{m}^3$ for piezoresistive sensing and $80 \times 40 \times 0.3 \mu\text{m}^3$ for piezoelectric sensing) greatly improve the figure-of-merit (FOM, defined to be the product of sensitivity and the square of fundamental resonant frequency) of the Y-axis acceleration sensitivity of the gyroscope. This is possible because the tiny sensing beams can be designed to be very flexible, since the vertical silicon beam is designed to be stiff enough to be the main contributor to the spring constant of the spring-mass model for the sensing mode vibration. The induced stress (on the tiny sensing beam) due to the sensing mode vibration is enhanced because of the extreme flexibility of the tiny sensing beam. Figure 3 shows the simulation results on this sensitivity improvement.

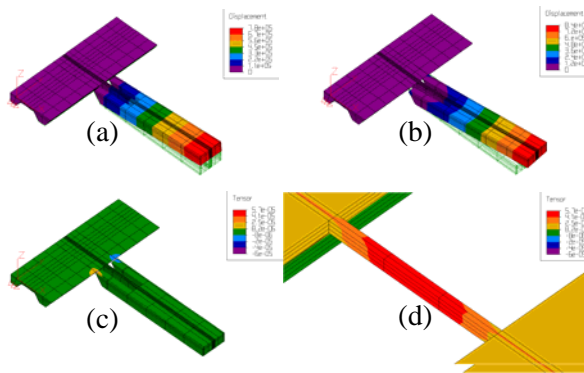


Figure 2. FEA simulations of (a) driving mode vibration; (b) sensing mode vibration; (c) stress distribution; (d) stress distribution on the sensing beam (all for the piezoresistive sensing gyroscope with small proof mass)

3. FABRICATION PROCESS

The main fabrication process is described in Figure 4. Silicon on insulator (SOI) n-type wafer and double-side-polished silicon wafer are used for the piezoresistive and piezoelectric sensing gyroscope, respectively. The wafers are first deposited with $0.4 \mu\text{m}$ thick low-pressure chemical vapor deposition (LPCVD) silicon nitride. Then, KOH anisotropic wet etching is performed from the backside to form the

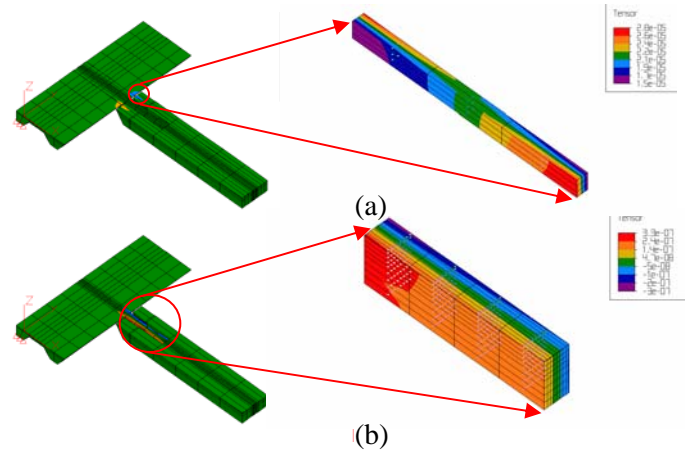


Figure 3. FEA simulations showing the Figure-of-Merit improvement by incorporating tiny sensing beams separate from the vertical support beam: (a) design with tiny sensing beams placed next to a vertical support beam; (b) design with only a vertical support beam. Both devices are designed with the same sensing-mode resonant frequency of 5.46kHz . The induced-stress simulations show that for a same applied Y-axis acceleration, the (a) design shows an induced stress level that is two orders of magnitude larger than the (b) design

backside to form the driving and sensing beam gap. Boron ion implantation is followed to form the piezoresistors at the front side for the piezoresistive sensing gyroscope, followed by Al-ZnO-Al depositions to form the sensing elements for piezoelectric sensing gyroscope. Then, a 3 μm thick ZnO layer, as well as the Al electrodes, is deposited to form the piezoelectric unimorph driving beam. After depositing parylene for the support layer, deep reactive ion etching (DRIE) is performed to etch through the 400 μm silicon wafer and release the device.

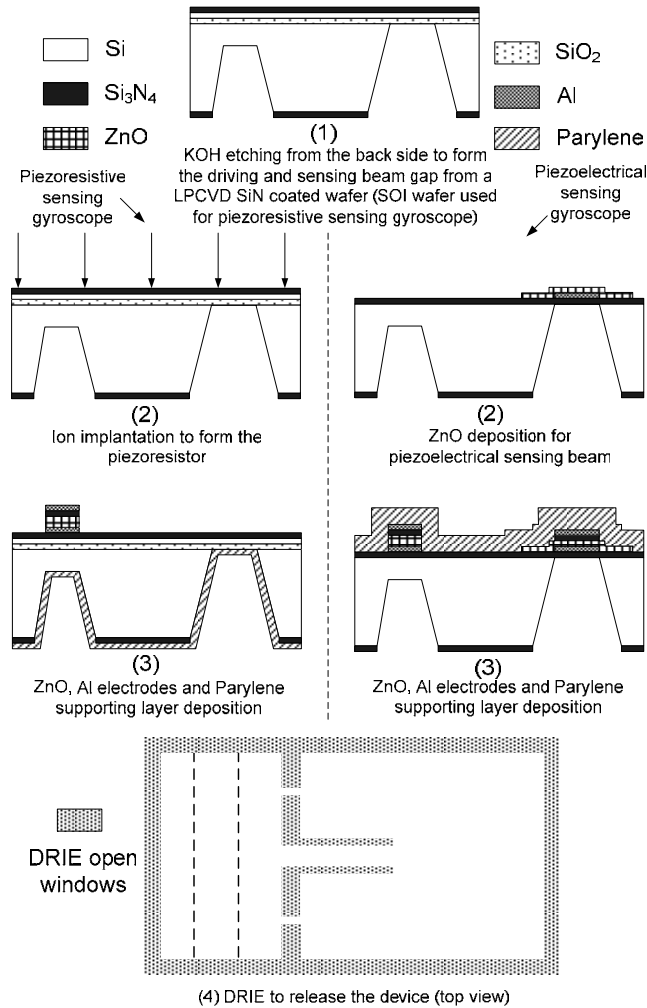
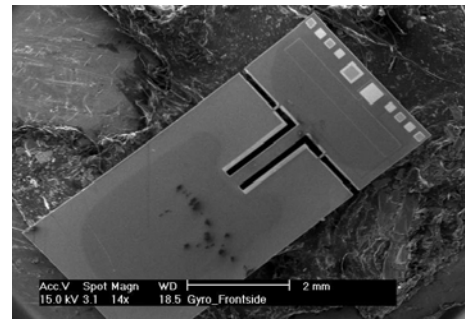
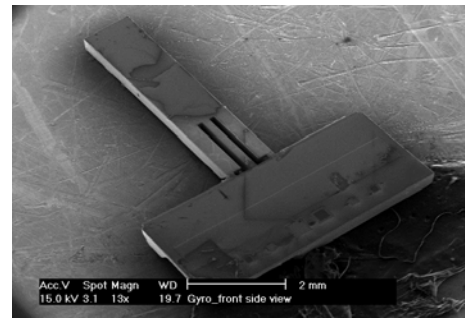


Figure 4. Brief fabrication process for the gyroscopes

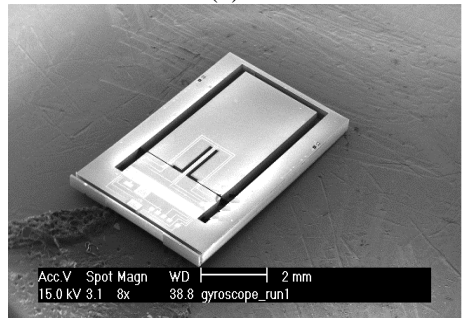
SEM pictures of the fabricated gyroscopes are shown in Figure 5 (a-d). Two different sizes of proof mass are fabricated. One is 3000x3000x400 μm^3 ; another is 3000x1000x400 μm^3 . A close-up view on the tiny sensing beam for the piezoesistive sensing gyroscope is also shown.



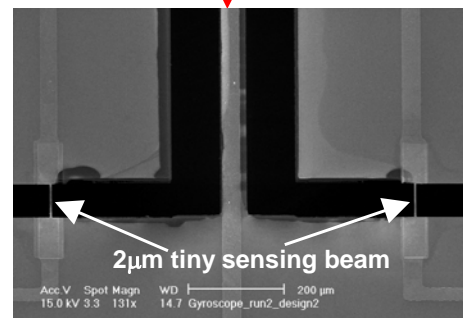
(a)



(b)



(c)



(d)

Figure 5. SEM Photos of the fabricated gyroscopes: (a) piezoelectric sensing gyroscope with large proof mass; (b) piezoelectric sensing gyroscope with small proof mass; (c) piezoresistive sensing gyroscope with large proof mass; (d) close-up view near the tiny sensing beams for the gyroscope in (c)

4. EXPERIMENT RESULTS

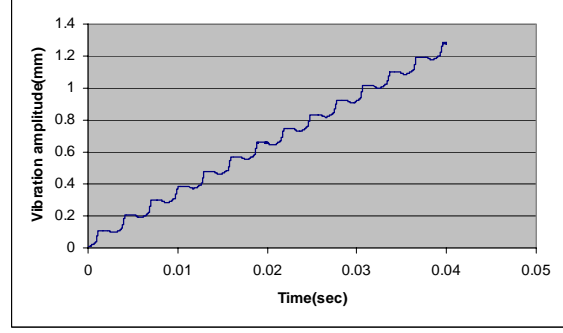
A laser vibrometer is used to measure the driving mode vibration amplitude. When we apply $32 \text{ V}_{\text{peak-to-peak}}$ sinusoidal signal to the piezoelectric unimorph of the gyroscope fabricated with the larger proof mass, we measure $116.2\mu\text{m}$ peak-to-peak displacement at its driving-mode resonant frequency of 1.34kHz (with a quality factor (Q) of 185). In the case of the gyroscope with the smaller proof mass, we observe a peak-to-peak driving-mode displacement of $43.3\mu\text{m}$ at its resonant frequency of 3.94kHz (with Q of 225). See Figure 6 (a-d).

We have applied Y-axis acceleration to the gyroscope to simulate the Coriolis force (that would be produced due to an applied angular rate). A Wheatstone bridge (or a voltage amplifier) is used to pick up the output from the piezoresistive (or piezoelectric) sensing gyroscope, as shown in Figure 7.

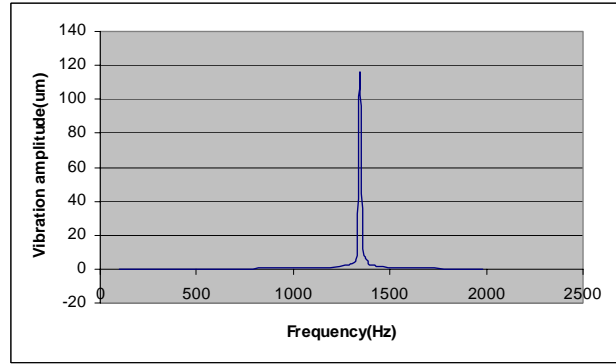
Figure 8 shows the gyroscope output response to the Y-direction acceleration. A standard accelerometer ADXL202 is used to calibrate the acceleration produced by the shaker. The unamplified Y-axis acceleration sensitivity of the piezoelectric sensing gyroscope is measured to be 200mV/g at 3.6kHz . For the piezoresistive sensing gyroscope, the Y-axis acceleration sensitivity is measured to be 3.36mV/g/V , which would lead to a minimum detectable X-axis angular rate of $0.086^\circ/\text{sec}$ at 1.32kHz as explained below:

Since the input referred noise for piezoresistive sensing gyroscope is $40\sim 60\mu\text{V}$, the minimum detectable Y-axis acceleration is $\frac{0.06\text{mV}}{3.36\text{mV/g/V} \cdot 15.34\text{V}} = 1.16 \times 10^{-3} g$. This excellent sensitivity is possible due to a two-orders-of-magnitude improvement of the figure-of-merit, as described earlier.

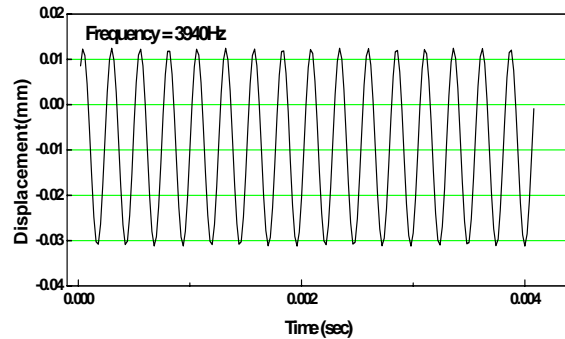
At an operating frequency ($\omega_d = \omega_y$) of 1.32kHz (20Hz away from the fundamental resonant frequency) that gives 1.5% Manufacturing tolerance, the driving-mode displacement drops from $116.2\mu\text{m}$ to $4.94\mu\text{m}$ ($=2A_d$). Thus, the sensing mode vibration amplitude (A_s) with the sensing mode Q_y of 185 is:



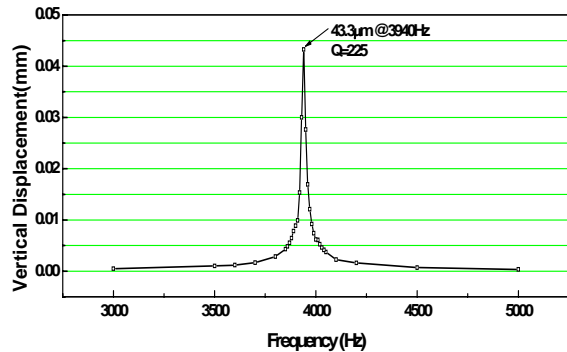
(a) Vibration displacement of the Figure 5 (c) gyroscope at 1.34kHz ($116.2\mu\text{m}$ peak-to-peak)



(b) Frequency Response of the Figure 5 (c) Device



(c) Vibration displacement of the Figure 5 (b) gyroscope at 3.94kHz ($43.3\mu\text{m}$ peak-to-peak)



(d) Frequency response of the Figure 5 (b) device

Figure 6. Drive-mode vibrations of the two gyroscopes measured by a laser vibrometer. The large displacement in (a) shows the laser vibrometer's drift in time

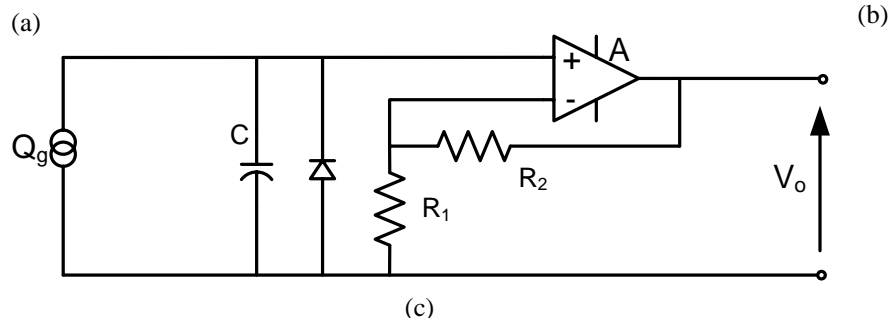
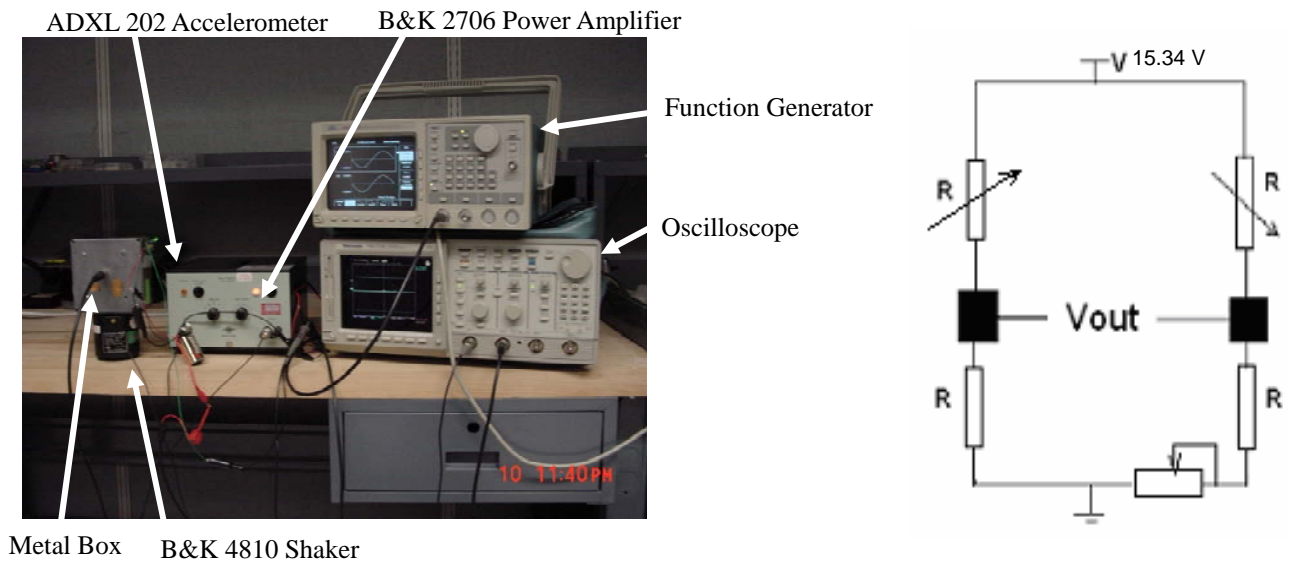


Figure 7. (a) Testing set-up (b) wheatstone bridge used for the piezoresistive-sensing gyroscope (c) voltage amplifier used for the piezoelectric-sensing gyroscope

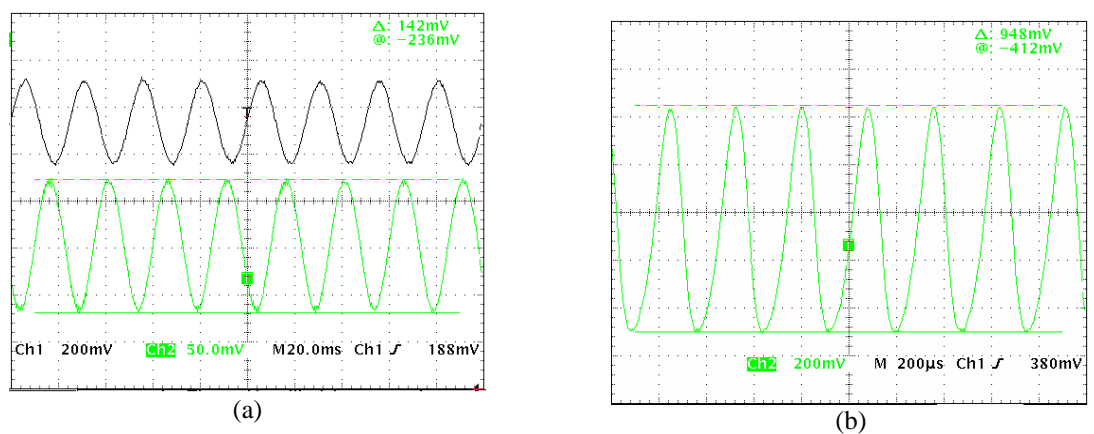


Figure 8. Typical outputs from the gyroscopes (green) and accelerometer ADXL202 (black) for a sinusoidal acceleration applied along the Y-axis: (a) the output of the piezoresistive sensing gyroscope to an applied 40Hz sinusoidal acceleration; (b) the output of the piezoelectric sensing gyroscope to an applied 3.6kHz sinusoidal acceleration

$$\frac{2A_d \omega_d \Omega}{\omega_y^2 \sqrt{[1 - (\omega_d / \omega_y)^2]^2 + [\omega_d / (\omega_y Q_y)]^2}} = 1.1 \times 10^{-7} \cdot \Omega. \tag{1}$$

Since the acceleration caused by Coriolis force is $A_s \omega_d^2$, the minimum detectable angular rate is:

$$\frac{1.16 \times 10^{-3} g}{1.1 \cdot 10^{-7} \cdot (2\pi \times 1320)^2} = 0.086 \text{ } ^\circ/\text{sec} \quad (2)$$

The measured linearity and frequency response of the piezoresistive sensing gyroscope for Y-axis acceleration are shown in Figure 9.

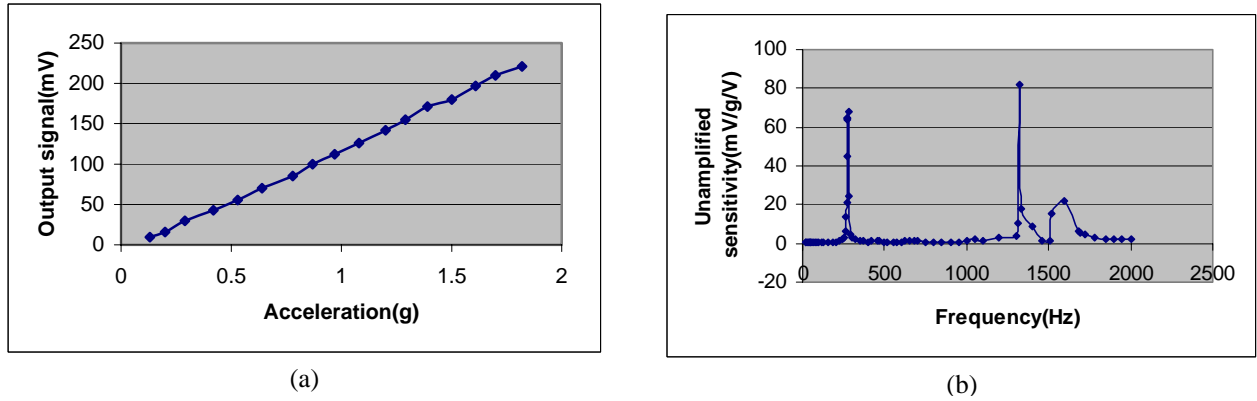


Figure 9. (a) linearity and (b) frequency response of the piezoresistive sensing gyroscope for a Y-axis acceleration

CONCLUSION

Piezoelectrically actuated gyroscopes with a novel sensing beam topology on a silicon chip are reported. Though the gyroscopes operate in air in atmospheric pressure with a relatively low Q, the sensitivity is very high, because of: 1) the very large vertical displacement (obtained by piezoelectric actuation) and 2) the tiny-sensing beams separated from the vertical-support beam that increases the FOM of the Y-axis acceleration sensitivity by two orders of magnitude. Thus, the driving-mode and sensing-mode frequencies do not have to be matched very tightly, and the gyroscope can be very competitive for automotive applications due to lower manufacturing costs.

REFERENCES

- [1] Madni, A.M., Costlow, L.E, "A third generation, highly monitored, micromachined quartz rate sensor for safety-critical vehicle stability control", *Aerospace Conference, 2001, IEEE Proceedings*. Volume 5, 10-17. March 2001 Page(s):2523 - 2534 vol.5.
- [2] Johnson, B., "Vibrating gyroscopes", *Moving and Flexing Microstructures - their Design, Modelling and Production, IEE Colloquium*, March 15, 1994, Page(s):3/1 - 315.
- [3] Qiang Zou, "Silicon MEMS Inertial Sensors for Biomedical and Automobile Application", *Ph.D. Dissertation*, University of Southern California, Los Angeles, CA, 2005.
- [4] Sharma, A., Zaman, F.M., Amini, B.V., Ayazi, F., "A high-Q in-plane SOI tuning fork gyroscope" *Sensors, 2004. Proceedings of IEEE*, October 24-27, 2004, Page(s):467 - 470 vol.1.
- [5] Yong Chen, Jiwei Jiao, Linxi Dong, Bin Xiong; Lufeng Che, Xinxin Li, Yuelin Wang, "Micromachined bar-structure gyroscope with high Q-factors for both driving and sensing mode at atmospheric pressure" *Sensors, 2003. Proceedings of IEEE*, Volume 1, October 22-24, 2003, Page(s):461 - 465 Vol.1.
- [6] Guohong He, Najafi, K., "A single-crystal silicon vibrating ring gyroscope" *Micro Electro Mechanical Systems, 2002, The Fifteenth IEEE International Conference*, January 20-24, 2002 Page(s):718 - 721.
- [7] Acar, C., Shkel, A.M., "An approach for increasing drive-mode bandwidth of MEMS vibratory gyroscopes" *Microelectromechanical Systems Journal*, Volume 14, Issue 3, June 2005 Page(s):520 - 528.